Title: Genetic and functional odorant receptor variation in the Homo lineage

Authors: Claire A. de March [1*†], Hiroaki Matsunami [1,2] Masashi Abe [1,3], Matthew Cobb [4], Kara C. Hoover [5*†]

Affilations:
[1] Department of Molecular Genetics and Microbiology, Duke University Medical Center, Durham, NC 27710, USA
[2] Department of Neurobiology, Duke Institute for Brain Sciences, Duke University, Durham, NC 27710, USA
[3] Department of Biotechnology and Life Science, Tokyo University of Agriculture and Technology, Tokyo 184-8588, Japan
[4] Faculty of Life Sciences, The University of Manchester, Oxford Road, Manchester, M13 9PL, USA
[5] Department of Anthropology, University of Alaska Fairbanks, Fairbanks Alaska, 99775, USA

* Corresponding authors (kchoover@alaska.edu, claire.de.march@duke.edu)
† These authors contributed equally to this work”

Abstract:.
Using ancient DNA sequences, we explored the function of olfactory receptor genes in the genus Homo. Humans, Neandertals, and Denisovans independently adapted to a wide range of geographic environments and the odours produced by their food. Variations in their odorant receptor protein sequence and structure resulted in variation in detection and perception. Studying thirty olfactory receptor genes, we found our relatives showed highly conserved receptor structures, but Homo sapiens did not. Variants led to changes in sensitivity to some odors, but no change in specificity, indicating a common olfactory repertoire in our genus. Diversity of geographic adaptations in H. sapiens may have produced greater functional variation in our lineage, increasing our olfactory repertoire and expanding our adaptive capacity.

One-Sentence Summary:
Using ancient DNA we studied the sense of smell in our extinct ancestors and in our relatives, Denisovans and Neanderthals

Main Text:

Terrestrial animals smell by binding odorant molecules to odorant receptors (ORs) but there is limited knowledge of odorant-OR and genotype-phenotype associations. Variation in mammalian ORs is strongly linked to ecological and dietary niche (1, 2). The human genus Homo underwent the most radical ecological niche expansion of all primates when migrating out of Africa and adapting to diverse global environments (3). Denisovans and Neandertals ancestors dispersed from Africa earlier than present-day humans (4) (~750,000 versus 65,000 years ago) and separated from each other ~300,000 years ago (5) (Fig. S1). Neandertals were geographically wide-ranging (western Europe, Middle East, Asia) while Denisovans were geographically constrained to Siberia (6, 7), the Tibetan plateau (8), and possibly beyond Wallace's Line (9). Olfactory stimuli from divergent environments following independent dispersals from Africa may have left traces of variation in Homo ORs. Among present-day humans, changes in OR function are linked to major evolutionary dietary shifts, such as scavenging, hunting, animal milk consumption, cooking, domestication (1, 10-14). But, what about the gap between Homo migrations and human-specific changes in ORs?

Using published ancient DNA sequences to analyze genetic variation for population structure and test functional differences in gene variants for ecological differentiation, we assess whether there is a shared Homo olfactory repertoire (range of detectable odors). We previously explored genetic and functional variation in present-day humans, Altai Neandertal, and Denisovan for OR7D4 (15). We extended our study to 29 additional open reading frames (Table S1) for ORs with known human receptor-odor (16, 17) and two additional Neandertals (Chagyrskaya, Vindija) and one ancient human (Ust'-Ishim) who lived in the same Altai montane locality (Table S2). We used 1000 Genomes for present-day humans (Table S3) (6). We found that novel variants alter sensitivity but not specificity of OR function and conclude that the olfactory repertoires of extinct lineages were highly overlapping. We also argue that expansion of the human olfactory repertoire occurred after our split with other migratory members of our genus.

Results

Genetic variation. Extinct lineages and Ust'-Ishim had fewer DNA and protein variants than 1000 Genomes (Fig. 1, Table S4)—on average 0.19% of nucleotides across 17 genes (or 0.11% when dividing across all 30 genes, including those matching the human wild type) compared to 0.82% of nucleotides across 30 genes in 1000 Genomes. Ancient populations were more prone to genetic drift (fixation and loss) due to smaller effective population sizes and living in small, isolated communities (18). Extinct lineages exhibit a pattern of OR gene conservation and present-day humans exhibit a pattern of tolerating variation.

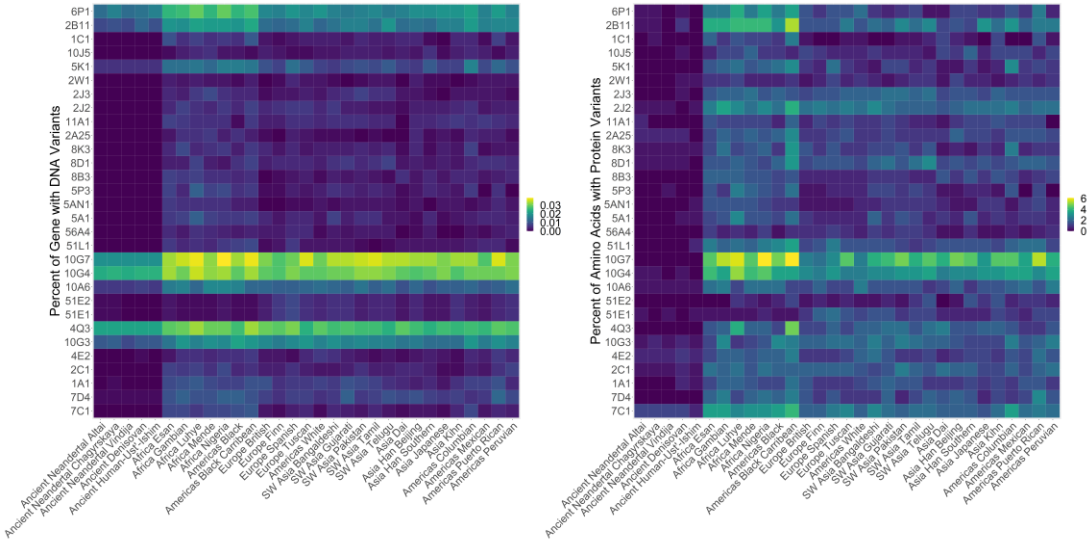

Fig. 1. Percent OR variation. Total variant count per gene divided by total basepairs in gene for each population and based on raw counts for ancient populations and raw count for the consensus sequence of each gene for each of 26 groups in 1000 Genomes.

The fixation index (Fst) measures genetic variance due to population structure (typically weighted by population size) and ranges from 0 (no differentiation) to 1 (complete differentiation) (19). The Fst values by gene for 1000 Genomes populations are lower than other large-bodied mammals with wide geographic dispersal (Table S5) (20). OR5P3 fixation was the highest at 11.4%, the lower limit of possible significant differentiation by population structure. The 1000 Genomes populations are not highly differentiation based on the 30 ORs used in this study an Fst mean of 4%. In contrast, the genus Homo (1000 Genomes and ancient samples) has an Fst mean of 11%, the lower end of possible significant differentiation by population structure. There was variation among Fst by gene, however. Ten Fst values were <1% (OR2W1, OR2J2, OR4Q3, OR5K1, OR6P1, OR7D4, OR8B3, OR10G7, OR11A1, OR51L1), which suggests the sort of random distribution associated with panmixia or genetic conservation. Of the 13 genes with Fst > 12%, seven were >20% (1C1, 5AN1, 7C1, 10G3, 10J5, 51E1, 51E2), which suggests the sort of distribution associated with high population differentiation. Of the genes with high Fst, only two had novel variants in extinct populations, which suggests that the small number of novel variants are not highly influential in differentiating populations (Table S7). The greater number of genes with high Fst indicate that Homo used to be more structured by population than present-day humans.

Looking at the distribution of variants, two ancient genes were identical to the human wild type (OR4Q3, OR8B3) and twenty contained variants also observed with 1000 Genomes—shared variation (Table S6), suggesting these variants occurred prior to global divergence of Homo. Only 11 genes, with a total of 14 variants, were unique to ancient samples (not found in 1000 Genomes). These genes may well be ones that were influenced by olfactory stimuli in divergent environments following dispersals from Africa. Denisovan had nine novel variants (of which two were synonymous) compared to the Neandertal five (of which 2 were synonymous). No novel variants were observed in the ancient human Ust'-Ishim.

Amino acid sequences for the ORs studied were used to form a cladogram to explore the relationships of our samples (Fig. S2). Extinct lineages formed a clade with Vindija Neandertal the most distinct, which was unexpected because genome-wide studies have indicated that Vindija is most genetically similar to Chagyrskaya Neandertal (18). The extinct clade was closest to the ancient human Ust'-Ishim and then to East and South Asian present-day humans—the latter groups harbor genetic signatures of introgression with Neandertals and Denisovans (9).

Functional Variation. Because gene function in not reliably predictable for ORs from sequence data (21, 22), we directly measured the functional responses of ORs containing novel variants. Each OR protein, expressed in a cell line, was screened against seven odorants previously identified in the literature as evoking responses: OR1A1 (21, 23), OR1C1 (22), OR2C1 (21), OR10J5 (21), OR5P3 (21), and OR10G3 (22). Dose response assays for the top screening responses included seven concentrations of the odors delivered separately.

There were only three Neandertal genes containing novel variants. Their dose responses were not correlated with those of present-day humans (Figs. 2A, 2C, 2D). Only 1C1 had a detectable response but significantly lower than that of present-day humans (Figs. 3A, 3C, 3D, 4, S2, S3). Despite the higher number of novel OR variants in the Denisovans and higher dose responses compared to present-day humans (Figs. 2C, 2D), the OR responses for six genes and those for human reference were significantly correlated (R2 = 0.87) (Fig. 2B). Tested Denisovan ORs were less sensitive to odors that present-day humans perceive as floral but much more sensitive to odors perceived as spicy, balsamic, or unpleasant (e.g., sulfur 4x greater and balsamic 3x greater than in present-day humans) (Table 1). Higher dose responses in Denisovan ORs appear to be driven by two amino acid variations in two of the ORs with novel variants (Fig. 3, Fig. S3).

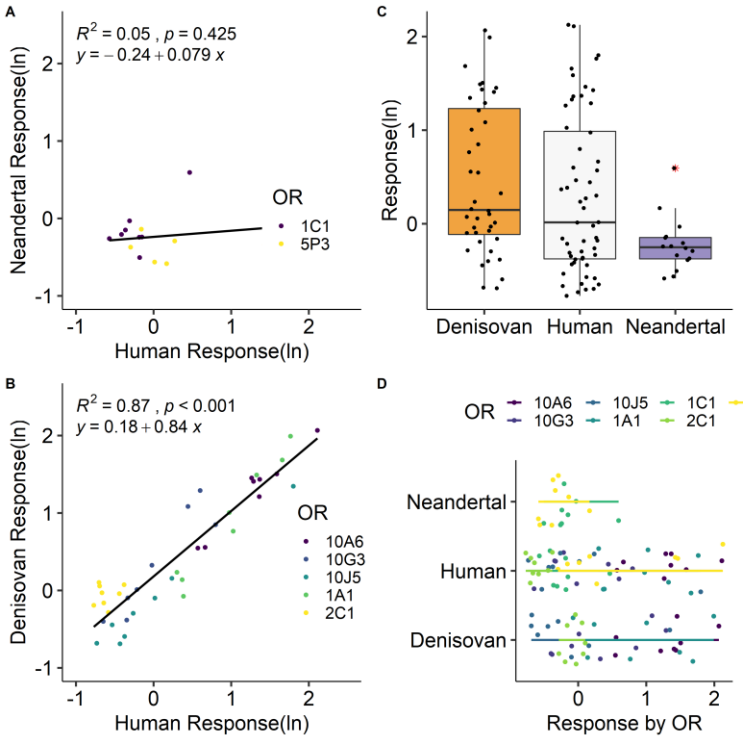

Fig. 2. Regression results for dose responses. A. Human and Denisovan, **B**. Human and Neandertal. **C**. Boxplots of dose responses for all samples showing median, box boundaries (first

and third quartiles), and two whiskers (upper whisker extends to the largest value no further than 1.5 inter-quartile range from third quartile; lower whisker extends to the smallest value at most 1.5 inter-quartile range of first quartile, outliers identified with red asterisk), **D**. Activity Indesx by OR for all three samples.

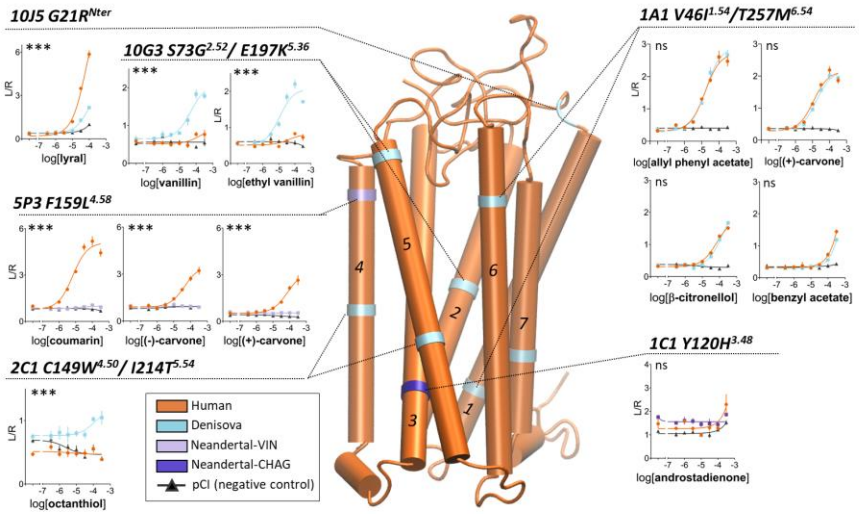

Fig. 3: Homology model of the human consensus odorant receptor. To illustrate location of variants, panels show dose-response for odorants that were significantly activating ORs in screening. (FigS3; 10G3 and 2C1 both have one shared and one novel mutation). The x-axis of panels represents the odorant concentration (M) and the y-axis the normalized luminescence generated by the activated OR. Error bars are SEM (standard error of the mean).

Despite using the same DNA sequence as previous studies of 2B11 (22) and 6P1 (17), the human reference for both did not respond to any of the ~350 odors (100µM) against which they were tested (Fig. S4)—neither did the extinct linages. In previous studies, OR2B11 (22) and OR6P1 (17) responded strongly to coumarin and anisaldehyde, respectively, at concentrations higher than 100µM. We found that such concentrations often cause cell toxicity or OR non-specific cell responses.

OR1A1. All but 2-heptanone induced a response in the screening assay (Fig. S3A) and the highest responses were for honey (particularly for Denisovan) (Table 1, Fig. 3). Neither of the two Denisovan variants (V461I1.54, T257M6.54) were in an amino acid region critical for mammalian OR function nor were they involved in the odorant binding cavity—perhaps explaining their minimal functional impact.

OR1C1. The only significant response was from Chagyrskaya Neandertal to androstadienone (Fig. S3B) and it was weak (Table 1; Fig. 3). Chagyrskaya Neandertal 1C1 variant Y120H3.48 is part of the highly conserved MAY3.48DRY motif involved in the activation of mammalian ORs (Fig. 3, Fig. S3B), which might explain why this variant alters function.

OR2C1. Screening assay responses were strong but not statistically significant (Fig. S3A). The dose response assay for octanethiol produced a statistically significant response in the Denisovan

version of this OR (Table 1, Fig. 3). The shared C149W4.50 corresponds to the conserved W4.50. The W residue is highly conserved in GPCRs but less so in ORs (58%). The location of the novel Denisovan I214T5.54 in TM5 is below residues involved in canonical ligand binding cavity and it points into the receptor rather than the surface. In addition, prior functional tests for C149 found a similar response (17). The C149W allele may stop protein function and may have produced octanethiol-specific anosmia.

OR5P3. In the screening assay, Vindija Neandertal did not have a significant response but the human reference responded to five of the seven odorants (Fig. S3B). Vindija dose responses, which included higher concentrations of the top three responses for present-day humans (courmarin and both enantiomers of carvone), did not exceed control (Fig. 3). The cell surface expression for Vindija indicated that the OR proteins was present at the cell surface, albeit at a slightly lower level than that in present-day humans. Vindija F159L4.58 is in the extracellular part of TM4 (Fig. 3), near 4.53, which is involved in mouse OR trafficking (24). We observed slightly lower trafficking of the Vindija protein. A similar mutation (S155A4.56) in human OR1A2 decreases in vitro responses to (S)-(-)-citronellal (23). If OR5P3 F159L4.58 is involved in odorant binding, the mutation of this position from phenylalanine to leucine might prevent the π-π stacking interaction between the aromatic residue and coumarin. We conclude that the Vindija protein is not functional and this might be attributable to many potential reasons (a few examples are lack of odorant binding, or fail in activation mechanism, or fail to bind the G protein).

OR10G3. The screening assay revealed significant responses for all seven odors in the Denisovan OR and in the human reference (Fig. S3A). Denisovan variants had significantly stronger dose responses to vanillin and ethyl vanillin compared to present-day humans (Table 1; Fig. 3). Neither of the Denisovan variants (S73G2.52, E197K5.36) were located in conserved amino acid regions (Fig. 3). TM2 is not involved in odorant binding or receptor function, implying that S73G2.52 probably did not change the receptor response. TM5 (E197K5.36) forms part of the binding cavity but position 5.36 is located at the very limit of ECL2. K at this position is a rare residue in present-day human ORs (3.6%), suggesting a functional, adaptative reason for this change. The location of the variant suggests it may be involved in ligand entry.

OR10J5. There were three significant screening responses to lyral and helional and eugenol (Fig. S3A). The Denisovan response to top odor lyral was lower than that of the human reference (Table 1, Fig. 3). The G21RNter variant of 10J5 found in the Denisovan is located at the very end of the N terminal end, just before the start of TM1. The role of this region in OR function is undetermined.

Table 1. Comparison of OR activity index for human and extinct lineages. Color coding is from low (purple) to high (mustard).

Gene	Odorant	Odor Description	Olfactory Note	Denisova	Human
OR10G3	ethyl vanillin	vanilla, creamy, caramellic	balsamic	10.28	3.57
OR10G3	vanillin	vanilla, creamy, chocolate	balsamic	8.98	3.52
OR1A1	beta-citronellol	citronella, rose, leafy, oily petal	floral	9.03	7.52
OR1A1	benzyl acetate	floral, jasmin, fruity	floral	2.38	2.89
OR10J5	lyral	floral, muguet	floral	4.33	11.71
OR1A1	allyl phenyl acetate	honey, fruity, rum	fruity	13.87	13.12
OR1A1	citral	lemon, juicy, lemon peel	fruity	2.66	2.99
OR10G3	g-undecalactone	peach, creamy, coconut	fruity	1.56	0.94
OR1A1	(+)-carvone	mint, herbal, spearmint	green	10.29	10.64
OR1A1	1-heptanol	musty, leaf, violet, herbal, green	green	0.80	0.89
OR10J5	helional	fresh green, watery, ozone	green	1.80	1.53
OR10G3	eugenol	clove, spicy, woody	spicy	1.90	1.37
OR2C1	1,3-propanthiol	meaty, sulfurous	sulfur	0.97	0.71
OR2C1	2- propanthiol	cooked vegetable, mustard	sulfur	1.02	0.64
OR2C1	nonanthiol	sulfurous	sulfur	1.45	0.00
OR2C1	octanthiol	sulfurous	sulfur	4.65	0.94
				Chagyrskaya	**Human**
OR1C1	androstadienone	urine, sweating	animal	3.73	4.58
				Vindija	**Human**
OR5P3	(-)-carvone	spicy, bready, caraway	spicy	1.92	15.41
OR5P3	(+)-carvone	mint, herbal, spearmint	green	1.09	13.14
OR5P3	1-heptanol	musty, leaf, violet, herbal, green	green	1.22	1.32
OR5P3	1-hexanol	fusel, oily, fruity, green	green	1.14	1.73
OR5P3	acetophenone	pungent, hawthorn, almond, mimosa	floral	1.30	1.80
OR5P3	coumarin	hay, tonka	balsamic	2.00	26.41

Discussion

Ten novel missense variants were located in 8 genes (out of 30), with five being functionally different from present-day humans (1C1, 2C1, 5P3, 10G3, 10J5), one the same (1A1) and two without identifiable ligands (2B11, 6P1). Given the small percentage of genes with variants altering OR function, members of the genus Homo likely shared an olfactory repertoire, with Neandertals and Denisovans smelling the same range of odors we do but having different dose responses to those odors. When OR function was altered by a novel OR, the difference was in sensitivity rather than specificity. Novel Denisovan OR variants (1A1, 2C1, 10G3, 10J5) were twice as responsive as human equivalents to odors present-day humans perceive as spicy, balsamic, and unpleasant (Table 1), but not to odors perceived as floral. Novel Neandertal variants were three times less responsive than human ORs, including reduced responses to odors perceived as green, floral, and spicy (Table 1). There is some correlation in Neandertal skull morphology that suggests their olfactory bulbs were smaller than present-day humans (6), but the link between bulb size and olfactory acuity is unclear (25, 26).

The Denisovan ORs strong response to honey may be ecologically significant. Honey is the most energy-dense natural food and is a prized component of living hunter-gatherer diets (except where bees are rare or absent)—even great apes have a ‘honey tooth’ (27). Energy-dense foods like sugars are sought by larger-brained primates (28) and, based on oral microbiome data,

Neandertals and present-day humans share functional adaptations in nutrient metabolism including starch digestion that are not found in our closest ape relatives (29). The high response to vanilla odors suggests a potential response to sweet things—an odor-taste pairing common in present-day humans (30).

Local ecological adaptive pressures may have acted on ORs in extinct lineages to produce the few novel variants observed, but extinct lineages were less variable in OR genes and proteins compared to 1000 Genomes. While differences in sample sizes might account for some of the striking differences, the reduced variation is probably due to genetic drift effect or conservation. Small effective population sizes cause bottlenecks and small, isolated populations (18) are prone to genetic drift. Purifying selection has been observed in chimpanzee ORs compared to a mix of relaxed and positive selection in human ORs (31) and extinct lineages may also have been subject to this, as evidenced by fewer variants that mostly code for synonymous proteins (compared to protein variation in 1000 Genomes). The mean of Fst values across genes comparing 1000 Genomes to extinct lineaages (11%) is higher than those for 1000 Genomes population comparisons (4%), which suggests that there are structural differences between them and us that reflect both explanations—drift and conservation. Based on our data the last common ancestor shared by Homo (present-day humans, Neandertals, Denisova, and others) and Pan (chimpanzees, bonobos) had a conserved set of ORs. Present-day humans derived away from the pattern of conservation more recently, with evolutionary pressure toward increased missense variation.

Despite having a shared repertoire with Neandertals and Denisovans, present-day humans are novel in their highly variable OR repertoire which may reflect cultural adaptations following migrations from Africa. Relaxed selection on OR genes for groups no longer engaging in traditional lifestyles is possible (32). 1000 Genomes groups outside Africa are less variable in most OR genes than those in Africa and OR gene enrichment is observed in African hunter-gatherer groups (Hadza and Pygmies) but not African agricultural (Yoruba) and pastoral (Maasai) groups (33). Tanzanian Sandawe hunter-gatherers show no OR allelic enrichment, however, which undermines the case for relaxed selection (33). High allelic diversity and OR generalization on a broad scale may have functional implications, such as increasing the effective size of the olfactory repertoire (34). Understanding our unique OR allelic diversity is an important challenge.

Our data provide insights into how the dispersal of human lineages outside of Africa (Denisova, Neandertal, ancient human) may have affected olfactory gene repertoire and function. Understanding the evolutionary genetics and functional significance of observed OR allelic variability in and almong human populations and extinct relatives sheds light on the role of olfaction in key aspects of human culture, and perhaps our current success as a global species.

References and Notes

1. G. M. Hughes et al., The birth and death of olfactory receptor gene families in mammalian niche adaptation. Mol. Biol. Evol., msy028-msy028 (2018).
2. S. Hayden et al., Ecological adaptation determines functional mammalian olfactory subgenomes. Genome Res. 20, 1 - 9 (2010).
3. A. Varki, D. H. Geschwind, E. E. Eichler, Human uniqueness: genome interactions with environment, behaviour and culture. Nature Reviews Genetics 9, 749 (2008).

4. I. C. Winder et al., Evolution and dispersal of the genus Homo: A landscape approach. J Hum Evol 87, 48-65 (2015).
5. K. Prufer et al., The complete genome sequence of a Neanderthal from the Altai Mountains. Nature 505, 43-49 (2014).
6. Z. Jacobs et al., Timing of archaic hominin occupation of Denisova Cave in southern Siberia. Nature 565, 594-599 (2019).
7. E. I. Zavala et al., Pleistocene sediment DNA reveals hominin and faunal turnovers at Denisova Cave. Nature, (2021).
8. F. Chen et al., A late Middle Pleistocene Denisovan mandible from the Tibetan Plateau. Nature 569, 409-412 (2019).
9. G. S. Jacobs et al., Multiple Deeply Divergent Denisovan Ancestries in Papuans. Cell 177, 1010-1021.e1032 (2019).
10. F. Luca, G. H. Perry, D. R. A., Evolutionary Adaptations to Dietary Changes. Annu. Rev. Nutr. 30, 291-314 (2010).
11. Jeremy F. McRae et al., Identification of Regions Associated with Variation in Sensitivity to Food-Related Odors in the Human Genome. Curr. Biol. 23, 1596-1600 (2013).
12. S. R. Jaeger et al., A Mendelian trait for olfactory sensitivity affects odor experience and food selection. Curr. Biol. 23, 1601-1605 (2013).
13. J. F. McRae et al., Genetic Variation in the Odorant Receptor OR2J3 Is Associated with the Ability to Detect the “Grassy” Smelling Odor, cis-3-hexen-1-ol. Chem. Senses 37, 585-593 (2012).
14. K. Lunde et al., Genetic variation of an odorant receptor OR7D4 and sensory perception of cooked meat containing androstenone. PLoS One 7, e35259 (2012).
15. K. C. Hoover et al., Global survey of variation in a human olfactory receptor gene reveals signatures of non-neutral evolution. Chem. Senses 40, 481-488 (2015).
16. H. Zhuang, M. Chien, H. Matsunami, Dynamic functional evolution of an odorant receptor for sex-steroid-derived odors in primates. Proc Natl Acad Sci U S A 106, 21247 - 21251 (2009).
17. J. D. Mainland et al., The missense of smell: functional variability in the human odorant receptor repertoire. Nat Neurosci 17, 114-120 (2014).
18. F. Mafessoni et al., A high-coverage Neandertal genome from Chagyrskaya Cave. Proceedings of the National Academy of Sciences 117, 15132-15136 (2020).
19. S. Wright, The interpretation of population structure by f-statistics with special regard to systems of mating. Evolution 19, 395-420 (1965).
20. A. R. Templeton, Human Races: A Genetic and Evolutionary Perspective. American Anthropologist 100, 632-650 (1998).
21. H. Saito, Q. Chi, H. Zhuang, H. Matsunami, J. Mainland, Odor coding by a Mammalian receptor repertoire. Sci Signal 2, ra9 (2009).
22. K. A. Adipietro, J. D. Mainland, H. Matsunami, Functional evolution of mammalian odorant receptors. PLoS Genet. 8, e1002821 (2012).
23. K. Schmiedeberg et al., Structural determinants of odorant recognition by the human olfactory receptors OR1A1 and OR1A2. J. Struct. Biol. 159, 400-412 (2007).
24. K. Ikegami et al., Structural instability and divergence from conserved residues underlie intracellular retention of mammalian odorant receptors. Proc Natl Acad Sci U S A 117, 2957-2967 (2020).
25. M. Bastir et al., Evolution of the base of the brain in highly encephalized human species. Nature Communications 2, 588 (2011).
26. T. Weiss et al., Human Olfaction without Apparent Olfactory Bulbs. Neuron, (2019).

27. F. W. Marlowe et al., Honey, Hadza, hunter-gatherers, and human evolution. J. Hum. Evol. 71, 119-128 (2014).
28. N. J. Dominy, Ferment in the family tree. Proceedings of the National Academy of Sciences 112, 308-309 (2015).
29. J. A. Fellows Yates et al., The evolution and changing ecology of the African hominid oral microbiome. Proceedings of the National Academy of Sciences 118, e2021655118 (2021).
30. G. Wang, J. E. Hayes, G. R. Ziegler, R. F. Roberts, H. Hopfer, Dose-Response Relationships for Vanilla Flavor and Sucrose in Skim Milk: Evidence of Synergy. Beverages 4, 73 (2018).
31. Y. Gilad, O. Man, G. Glusman, A comparison of the human and chimpanzee olfactory receptor gene repertoires. Genome Research 15, 224-230 (2005).
32. M. Somel et al., A scan for human-specific relaxation of negative selection reveals unexpected polymorphism in proteasome genes. Mol. Biol. Evol. 30, 1808-1815 (2013).
33. J. Lachance et al., Evolutionary history and adaptation from high-coverage whole-genome sequences of diverse African hunter-gatherers. Cell 150, 457-469 (2012).
34. C. Trimmer et al., Genetic variation across the human olfactory receptor repertoire alters odor perception. Proceedings of the National Academy of Sciences, 201804106 (2019).
35. The Genomes Project Consortium, The 1000 Genomes Project Consortium. Nature 526, 68-74 (2015).
36. G. M. Hughes, E. C. Teeling, D. G. Higgins, Loss of olfactory receptor function in hominin evolution. PLOS ONE 9, e84714 (2014).
37. K. Prüfer et al., A high-coverage Neandertal genome from Vindija Cave in Croatia. Science, (2017).
38. F. Mafessoni et al., A high-coverage Neandertal genome from Chagyrskaya Cave. bioRxiv, (2020).
39. L. L. Prieto-Godino et al., Olfactory receptor pseudo-pseudogenes. Nature 539, 93-97 (2016).
40. I. H. Barnes et al., Expert curation of the human and mouse olfactory receptor gene repertoires identifies conserved coding regions split across two exons. BMC Genomics 21, 1-15 (2020).
41. P. Danecek et al., The variant call format and VCFtools. Bioinformatics 27, 2156-2158 (2011).
42. P. Danecek, S. A. McCarthy, BCFtools/csq: haplotype-aware variant consequences. Bioinformatics 33, 2037-2039 (2017).
43. R. C. Team. (2021).
44. H. Wickham et al. (2019).
45. H. F. Wickham, Romain; Henry, Lionel; Müller, Kirill, in R package version 1.0.7. (2021).
46. H. Wickham, The tidyverse. R package ver 1, 836 (2017).
47. H. Pagès, P. Aboyoun, R. Gentleman, S. DebRoy, Biostrings: Efficient manipulation of biological strings. R package version 2, 10.18129 (2019).
48. B. Auguie, A. Antonov, M. B. Auguie, Package ‘gridExtra’. Miscellaneous Functions for “Grid” Graphics, (2017).
49. S. R. Gadagkar, M. S. Rosenberg, S. Kumar, Inferring species phylogenies from multiple genes: concatenated sequence tree versus consensus gene tree. Journal of Experimental Zoology Part B: Molecular and Developmental Evolution 304, 64-74 (2005).
50. E. Paradis, J. Claude, K. Strimmer, APE: analyses of phylogenetics and evolution in R language. Bioinformatics 20, 289-290 (2004).

51. D. Charif, J. R. Lobry, in Structural approaches to sequence evolution. (Springer, 2007), pp. 207-232.
52. S. P. Wilkinson, S. K. Davy, phylogram: an R package for phylogenetic analysis with nested lists. Journal of Open Source Software 3, 790 (2018).
53. X. Zheng, M. X. Zheng, Package ‘gdsfmt’. (2014).
54. X. Zheng, M. X. Zheng, Package ‘SNPRelate’. A package for Parallel Computing Toolset for Relatedness and Principal Component Analysis of SNP Data, (2013).
55. T. Galili, dendextend: an R package for visualizing, adjusting and comparing trees of hierarchical clustering. Bioinformatics 31, 3718-3720 (2015).
56. C. Bushdid, C. A. de March, H. Matsunami, J. Golebiowski, in Olfactory Receptors: Methods and Protocols, F. M. Simoes de Souza, G. Antunes, Eds. (Springer New York, New York, NY, 2018), pp. 77-93.
57. TheGoodScentsCompany. (2021), vol. 2021.
58. C. A. de March, S.-K. Kim, S. Antonczak, W. A. Goddard, J. Golebiowski, G protein-coupled odorant receptors: From sequence to structure. Protein Science 24, 1543-1548 (2015).
59. M. L. Delignette-Muller, C. Dutang, fitdistrplus: An R package for fitting distributions. Journal of statistical software 64, 1-34 (2015).
60. J. Fox et al., Package ‘car’. Vienna: R Foundation for Statistical Computing, 16 (2012).
61. H. Wickham, ggplot2. Wiley Interdisciplinary Reviews: Computational Statistics 3, 180-185 (2011).
62. A. Kassambara, M. A. Kassambara. (2020).
63. C. O. Wilke, H. Wickham, M. C. O. Wilke, Package ‘cowplot’. Streamlined Plot Theme and Plot Annotations for ‘ggplot2, (2019).

Acknowledgments: The high-performance computing and data storage resources operated by the Research Computing Systems Group at the University of Alaska Fairbanks, Geophysical Institute.

Funding: Provide complete funding information, including grant numbers, complete funding agency names, and recipient's initials. Each funding source should be listed in a separate paragraph.
US National Science Foundation Award 1550409 (KCH)
National Institutes of Health grant K99DC018333 (CADM)
US National Science Foundation Award 1556207 (HM)
National Institutes of Health grant DC014423 (HM)
National Institutes of Health grant DC016224 (HM)

Author contributions:

Conceptualization: KCH, HM, MC

Methodology: KCH, CADM, HM, MC

Investigation: KCH, CADM, MA

Visualization: KCH, CADM

Funding acquisition: KCH, CADM, HM

Project administration: KCH, HM

Supervision: KCH, HM

Writing – original draft: KCH, CADM

Writing – review & editing: KCH, CADM, MC, HM

Competing interests: Authors declare that they have no competing interests.

Data and materials availability:
Data Availability. Raw data for this project and data derived from it are available in at *https://github.com/kchoover14/OldNoses* and are usable under the license provided in the repository.
Code Availability. Code for VCF data scraping and code for analysis in Tables S4-S5 and Figs. 1-2 and Figs. S1-S2, S7-S9 are available at *https://github.com/kchoover14/OldNoses* and are usable under the license provided in the repository.

Supplementary Materials

Materials and Methods

Figs. S1 to S9

Tables S1 to S9

References (*35*–*63*)

Science
AAAS

Supplementary Materials for

Genetic and functional odorant receptor variation in the Homo lineage

Claire A. de March, Hiroaki Matsunami, Masashi Abe, Matthew Cobb, Kara C. Hoover
Correspondence to: kchoover@alaska.edu, claire.de.march@duke.edu

This PDF file includes:

Materials and Methods
Supplementary Text
Figs. S1 to S9
Tables S1 to S9
Captions for Data S1

Materials and Methods

Materials

We cataloged variants in high quality paleogenomic sequence data produced by the Max Planck Institute Leipzig (Table S2) for Neandertals (Altai, Chagyrskaya, Mezmaiskaya), Denisovan 3 (the only high quality Denisovan genome, finger phalanx), and an ancient human hunter-gatherer from Siberia (Ust'-Ishim). We used the data generated by snpAD in /neandertal/vindija/vcf, an ancient DNA damage-aware genotyper.1 The VCF reference genome for genomes analyzed was hg19/GRCh37. Only variants with a minimum genotype quality of 20 (GC20) were used for downstream analysis. Our sample of present-day humans was from the 1000 Genomes dataset (35) consisting of over 2,500 individuals from 26 populations in Africa, the Americas, Europe, and Asia (Table S3). The 26 groups in 1000 Genomes were comprised of individuals with at least 3 out of 4 grandparents identifying membership in the group. While there are some groups engaging in pastoral or traditional horticulture/farming lifestyles, most practice mixed subsistence economies and lead western lifestyles. Although the draft genomes of Neandertals and Denisovans were reported as having more nonfunctional ORs than present-day humans (36), these genomes have since been revised (37, 38). The bioinformatic identification of olfactory pseudogenes has been experimentally challenged (39) by data showing the receptors containing coding sequence regions split into separate exons are conserved across mammals and expressed at the same level as protein-coding receptors with a single exon (40).

We focused on 30 OR genes shown to generate functional response data in previous studies (16) (Table S1). Gene regions were targeted using NCBI and RefSeq ranges—in the case of eight genes that contained up- and downstream sequences, the region was cut to the protein coding portion of the gene to be consistent with the other 22 genes that contained no up- or downstream areas.

Methods

Variant calling

Max Planck and 1000 Genomes Project both used the reference genome, hg19/GRCh37, to call variants using VCFtools (41). GRCh37 is built from sequences from different individuals and serves as the wild type relative. If the reference allele is C at a specific genomic position, a variant is called if it is not a C. We excluded insertions and deletions from analysis. BCFtools (42) was used to slice VCFs into chromosomes (ancient DNA) and genes of interest. For 1000 Genomes, BCF tools was also used to generate population specific VCF files. BCF tools was used to create consensus sequences for each gene for the entire 1000 Genomes dataset and for each population.

We cataloged variants using two sets of VCF data published by Max Planck Institute for Evolutionary Anthropology Leipzig in 2013 and 2016. Both datasets are based on the same

original sequence data but the 2016 VCFs were generated using snpAD, an ancient DNA damage-aware genotyper, and are more conservative estimates mutations (37).
The 2016 ancient VCFs (Table S2, S6) include high quality data from three Neandertals (Altai, Chagyrskaya, Vindija), lower quality data from one Neandertal (Mezmaiskaya), high quality from one Denisova (Denisovan 3), and one ancient human contemporary to Altai Neandertal and Denisova in Denisova Cave (Ust'-Ishim).

The 2013 VCF data analysis included high quality data—but not subject to the damage-aware genotyper—for Altai Neandertal, Denisova 3, and Ust'-Ishim. Variants were called using a custom bioinformations pipeline (Fig. S5). Data are found at http://cdna.eva.mpg.de/ust-ishim/VCF and http://cdna.eva.mpg.de/neandertal/altai/AltaiNeandertal/. Most variants were shared with present-day humans (Table S8). Three genes matched the human wild type (contained no variants, novel or shared) in all three samples tested (OR5K1, OR11A1, OR56A4) and 16 contained novel missense variants (Table S9). See Fig. S6 for functional results and Fig. S7 for regression results—Altai is significantly different from present-day humans and Denisova but there were few differences in terms of patterns of response.

Novel variant calling

R v4.1.0 (43) via R Studio v1.4.1717 (Rstudio, inc., Boston, MA, 2015) were used for analysis. Excel and csv files were read using readxl (44). The hash function in R used 1000 Genomes variant data (35) as a key to flag variants present in ancient samples but not found in present-day humans. Data were manipulated using dplyr (45) and tidyverse (46).

Genetic Analysis

Variants were called using DNAsp to generate Nexus files for each gene comparing a consensus sequence for each of the 26 groups in 1000 Genomes to the human reference sequence used for the published datasets (Max Planck and 1000 Genomes). Consensus sequences were used for each group in 1000 Genomes to reduce the sample size for comparison to ancient sequences which represented individuals, not groups. Biostrings (47) was used in R to create protein sequence files and call amino acid substitutions. Figures for percentage of variation by gene were generated using the R package ggplot2 with the viridis color-blind friendly palette and plotted panels using gridExtra (48). Concatenated amino acid sequences were used to infer phylogenetic relationships across populations for 30 genes (49). The phylogenetic tree was created using the R packages ape (50), seqinr (51), phylogram (52), gdsfmt (53), SNPrelate (54), and dendextend (55). Fst was calculated using gdsfmt (53) and SNPRelate (54) for Figs 1-2 and Figs S1-S2, S7-S9.

Primer design

ORs for extinct humans were created by mutating human ORs to match paleogenomic sequence data using

chimeric PCR. Forward and reverse PCR primers containing the desired mutation were designed to have a 56ºC or 58ºC annealing temperature, obtained from Integrated DNA Technologies, and diluted to 5µM.

Chimeric PCR

Chimeric PCR was performed using Phusion polymerase and Rho-tagged OR in a pCI vector as a template, with separate reactions using the forward primers paired with a 3' pCI primer or reverse primers paired with a 5' pCI primer (56). The reaction was started at 98ºC for 30 seconds, then run for 25 cycles of the following conditions: denaturation at 98ºC for 5 seconds, primer annealing at 55ºC for 15 seconds, and elongation at 72ºC for 30 seconds. The reaction was then held at 72ºC for 5 minutes. The products resulting from the forward and reverse primers were combined for each mutant and diluted 10x with distilled water (Gibco). A second PCR was performed using Phusion polymerase, 5' and 3' pCI primers, and the combined and diluted products for each desired mutant as the template. The same PCR conditions were used. The products were purified using the QIAquick PCR Purification Kit (Qiagen), cut with MluI and NotI restriction enzymes, run on a 1.1% agarose gel with GelRed, and extracted using the QIAquick Gel Extraction Kit (Qiagen). The products were then ligated into Rho-tagged pCI cut with MluI and NotI using T4 ligase (New England Biolabs) and used to transform competent ampicillin-resistant E. Coli. These were plated on LB-ampicillin plates and incubated at 37ºC overnight, then a single colony was grown in 4mL of 2XYT-ampicillin (100mg/mL) medium overnight at 37ºC. The Denville Miniprep Purification Kit was used to lyse the bacteria and purify the plasmid DNA. The concentration of the products was determined using an Eppendorf Biophotometer, and then adjusted to 100ng/µL using TE buffer. The products were sequenced using BigDye Terminator Sequencing Kit (Applied Biosystems), purified using Sephadex (GE Healthcare), and sequenced with 3130 Genetic Analyzer (Applied Biosystems).

Luciferase assay

Functionality was tested by a Luciferase assay as described in Zhuang and Matsunami (16). Hana3A cells were plated in Minimum Essential Medium (MEM) containing 10% FBS (vol/vol), penicillin-treptomycin and amphotericin B on Poly-D-lysine coated 96-well plates (Corning #3843) and co-transfected using Lipofectamine2000 (Invitrogen) with the prepared Rho-tagged OR or the empty vector pCI (negative control), RTP1S, and the muscarinic receptor M3. The cells were transfected with elements from the Dual-Glo Luciferase Assay System (Promega): the cAMP response element (CRE) coupled with a luciferase reporter gene (L); and the constitutively active SV40 promoter region coupled with the Renilla luciferase (RL) reporter. In a period of 18-24 hours after transfection, the medium was replaced with 0 µM, 1 µM, 3.16 µM, 10 µM, 31.6 µM, 100 µM, or 316 µM of odorants (Sigma Aldrich) in CD293 (Gibco) containing glutamine and copper and incubated for 3.5 hours. After the addition of Dual-Glo luciferase substrate and buffer (Promega), plates were read using BMG Labtech POLARStar Optima plate

reader. Promega Stop-and-Glo buffer and RL substrate were added, and plates were read again. The degree of activation was quantified for each well in Microsoft Excel using the formula (L-400)/(RL-400) and reported on the y axis (emitted in lumens). The RL quantification is made due to variation in cell numbers in each well and the 0µM values provide the basal activity value for each OR. 0µM thus served as a comparison to identify OR response values to odorant stimulations —if the odor value on the y-axis exceeded the 0µM value, the OR was taken to have responded to the odor but if the odor value did not exceed the 0µM value, the OR was considered unresponsive. Dose responses and EC50s were determined with Graphpad Prism 7. Activity index have been calculated from dose responses by multiplying the absolute value of the logEC50 to the efficacy. If EC50 could not be determined because the dose response did not reach its plateau, logEC50 were set as the arbitrary value -2. These values were used for Table 1 along with odor descriptors and olfactory notes from Good Scents (57).

Flowcytometry

The cell surface expression of the Rho-tagged ORs was evaluated as described in Ikegami, de March et al. (24). HEK293 cells were plated in 35 mm plates at 25% confluency and grown overnight at 37°C and 5% CO2. The cells were then transfected with the Rho-tagged ORs and GFP using the Lipofectamine2000 reagent (ThermoFisher Scientific) in MEM supplemented with 10% FBS. 18 to 24h later, the cells were detached from the plates with cellstripper and resuspended in PBS containing 15 mM NaN3, 2% FBS in ice. The cells were then centrifuged at 4°C and resuspended and incubated for at least 30min in primary antibody (mouse anti Rho4D2, Millipore Sigma). The cells were then centrifuged at 4°C and resuspended and incubated for at least 30 min and in the dark in phycoerythrin (PE)-donkey anti-mouse F(ab')2 Fragment antibody (Jackson Immunologicals: 715-116-150). Finally, the cells were stained with 7-Amino-actinomycin D (7AAD, Calbiochem). The cell surface expression was monitored through the PE fluorescence emitted by cells GFP positive, single, spherical, viable and 7AAD negative using a BD FACSCanto II. The results were analyzed with Flowjo. Olfr539 and Olfr541 were added to the experiment plan as positive and negative, respectively, controls of OR cell surface expression.

Homology model

The protocol followed a previously published method (56). 391 human OR sequences were aligned to pre-aligned sequences of 11 GPCRs including bovine rhodopsin (PDB: 1U19), human chemokine receptors CXCR4 (PDB: 3ODU) and CXCR1 (PDB: 2LNL), and human adenosine a2A receptor (PDB: 2YDV) using Jalview (58). The four experimental GPCR structures (1U19, 3ODU, 2YDV and 2LNL) were used as templates to build the human consensus OR by homology modeling with Modeller. The human consensus amino acid sequence was determined by aligning 391 human OR sequences and by selecting the most conserved amino acid for each position. Five models were obtained and the one fulfilling several constraints (binding cavity

sufficiently large, no large folded structure in extra-cellular loops, all TMs folded as α-helices, a small α-helix structure between TM3 and TM4) was retained for further structural analysis. Visualization of the models and picture generation were performed with VMD.

Regression Analysis

Data were analyzed in R for Windows 4.1.0, using the R Studio GUI for Windows 1.4.1717. Data were wrangled using dplyr (45) and tidyverse (46). The dose response dependent variable was fitted to distributions using fitdistrplus (59) and formed log normal distributions. The natural log was used to transform to normally distributed data for linear regression models. The car package (60) was used for ANOVA. 0μM values, as noted above, provided a control (the baseline threshold of OR activation). Because the number of cells varied across plates, the OR tested for each sample had a different 0μM. As such, removing values below the 0μM for each correlation between present-day humans and ancient DNA sample resulted in some odors missing values for one of the lineages. We compared the results of regression for testing using only active ORs (above the 0μM value) and for the full set of ORs—the results were nearly identical (Fig S8 for 2016 VCFs, Fig S9 for 2013 VCFs). Testing the full suite of responses, active or below the threshold, allowed a broader comparison of how these cells operate. Analysis was conducted on the full dataset for both between sample correlations and for mean difference testing. Plots for data visualization and results were created using ggplot2 (61) and ggpubr (62). Panels were created using cowplot (63) and ggarrange.

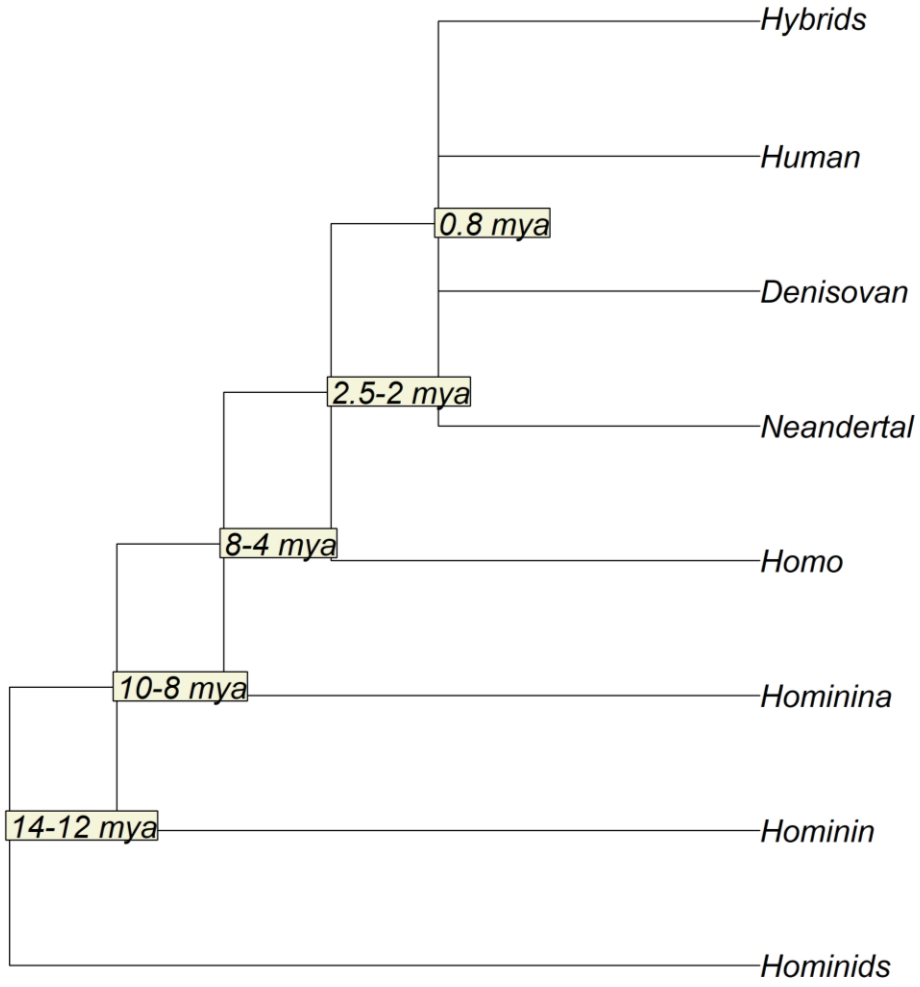

Fig. S1.
Phylogenetic tree of Hominids

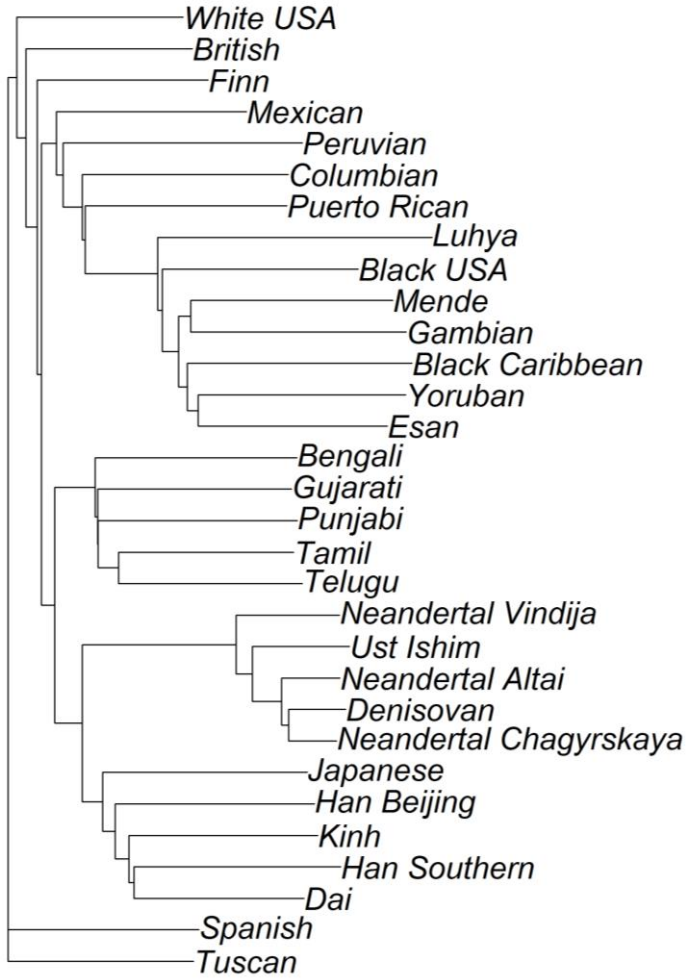

Fig. S2.
Cladogram based on full amino acid sequences for all 30 odorant receptors in ancient lineages and in 1000 Genomes populations.

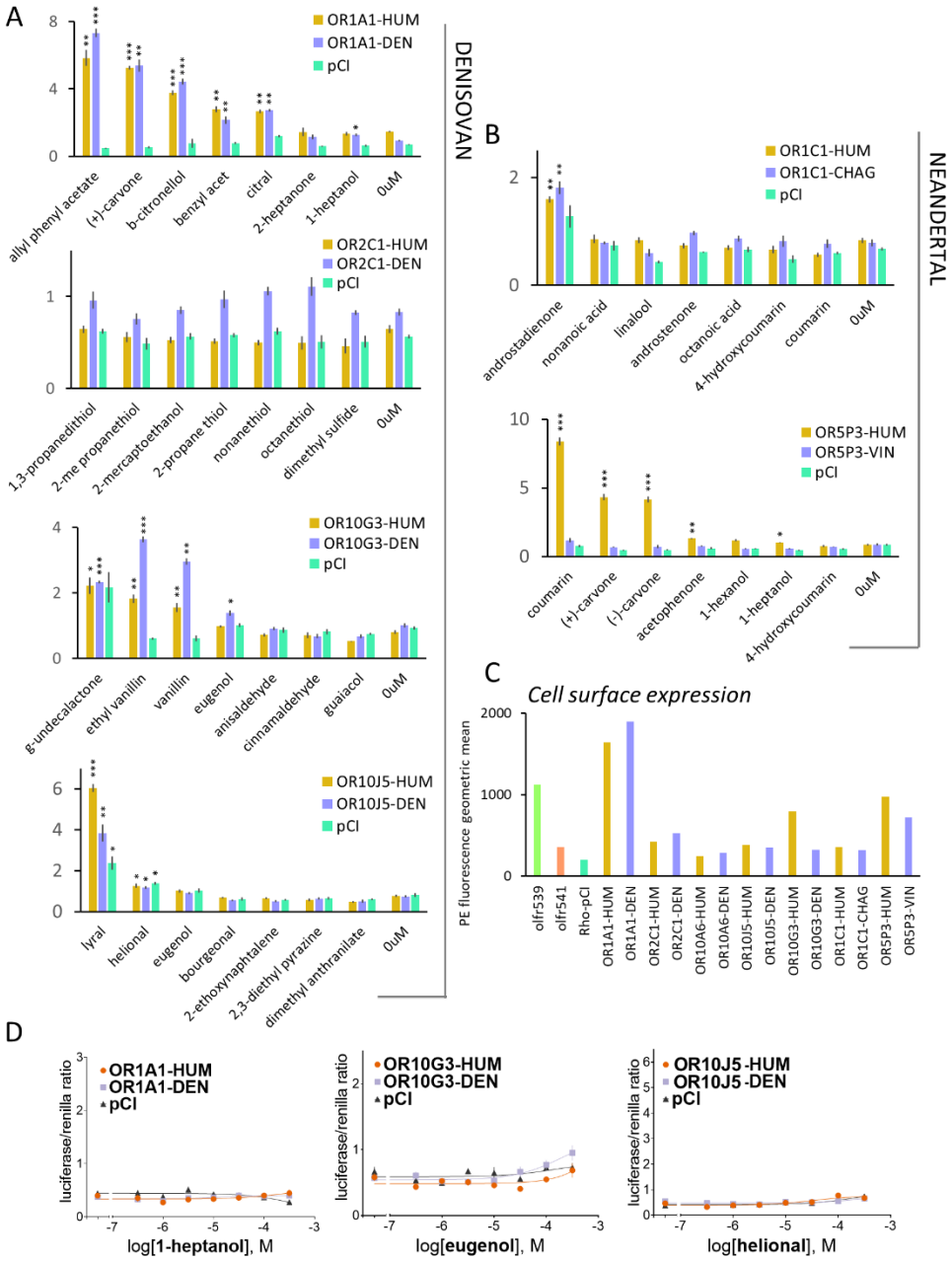

Fig. S3.

Functionality of hominin OR variants. Each Denisova (**A**) and Neandertal (**B**) OR response was first tested in luciferase assay against seven odorants (100µM) previously identified as evoking responses in human OR1A1 (21-23), OR1C1 (22), OR2C1 (21), OR10J5 (21, 22), OR5P3 (21, 22), and

OR10G3 (22). The empty vector pCI was added to each experiment as a control of OR-specific response. The y-axis represents the normalized luminescence as a measure of OR activation. Asterisks represent the level of significance in a paired t-test between the odorant stimulation and the no odor (0µM) control for each OR (* $p<0.05$; ** $p<0.01$; *** $p<0.001$). **C**. Cell surface expression of all OR variants. Olfr539 and Olfr541, served as positive and negative control of cell surface presence, respectively. **D.** Dose response of the false positives detected in the screening (**A**).

A
Toxic for cells
Tested in dose-response for OR2B11
Tested in dose-response for OR6P1
Screening

Fig. S4.
OR2B11 and OR6P1 response. **A.** Activation screening for OR2B11 and OR6P1 against more than 300 odorant molecules at 100 µM. **B**. List of odorants selected for validation by dose response. **C**. Dose-responses of OR2B11 to the odorants listed in **B**. **D.** Dose-responses of OR6P1 to the odorants listed in **B**. In panels **A**, **C** and **D** the y-axis represents the normalized luminescence response that is synonymous with OR activation.

```
# split bam into chromosomes, sort, and index
samtools view -b <filename_in>.bam <chromosome number> <filename_out>.bam
samtools sort -l 9 -O bam <filename_in>.bam -o <filename_out>.bam
# call variants, sort, and index
samtools index <filename_sorted>.bam
samtools mpileup -ufI <filename_RSfasta>.fa <filename_sorted>.bam > <filename>.bcf
bcftools view -vcg <filename_in>.bcf > <filename_out>.vcf
bgzip <filename>.vcf
tabix <filename>.vcf.gz
# extract gene interest, zip, and index
vcftools --gzvcf <filename>.vcf.gz --chr <#> --from-bp <#> --to-bp <#> --recode --recode-INFO-all --out
<filename>
bgzip <filename>.recode.vcf
tabix <filename>.recode.vcf.gz
# make fasta
cat <filename_RSfasta>.fa | vcf-consensus <filename_in>.recode.vcf.gz > <filename_out>.fa
```

Fig. S5.
Custom variant calling pipeline for data not in VCF format

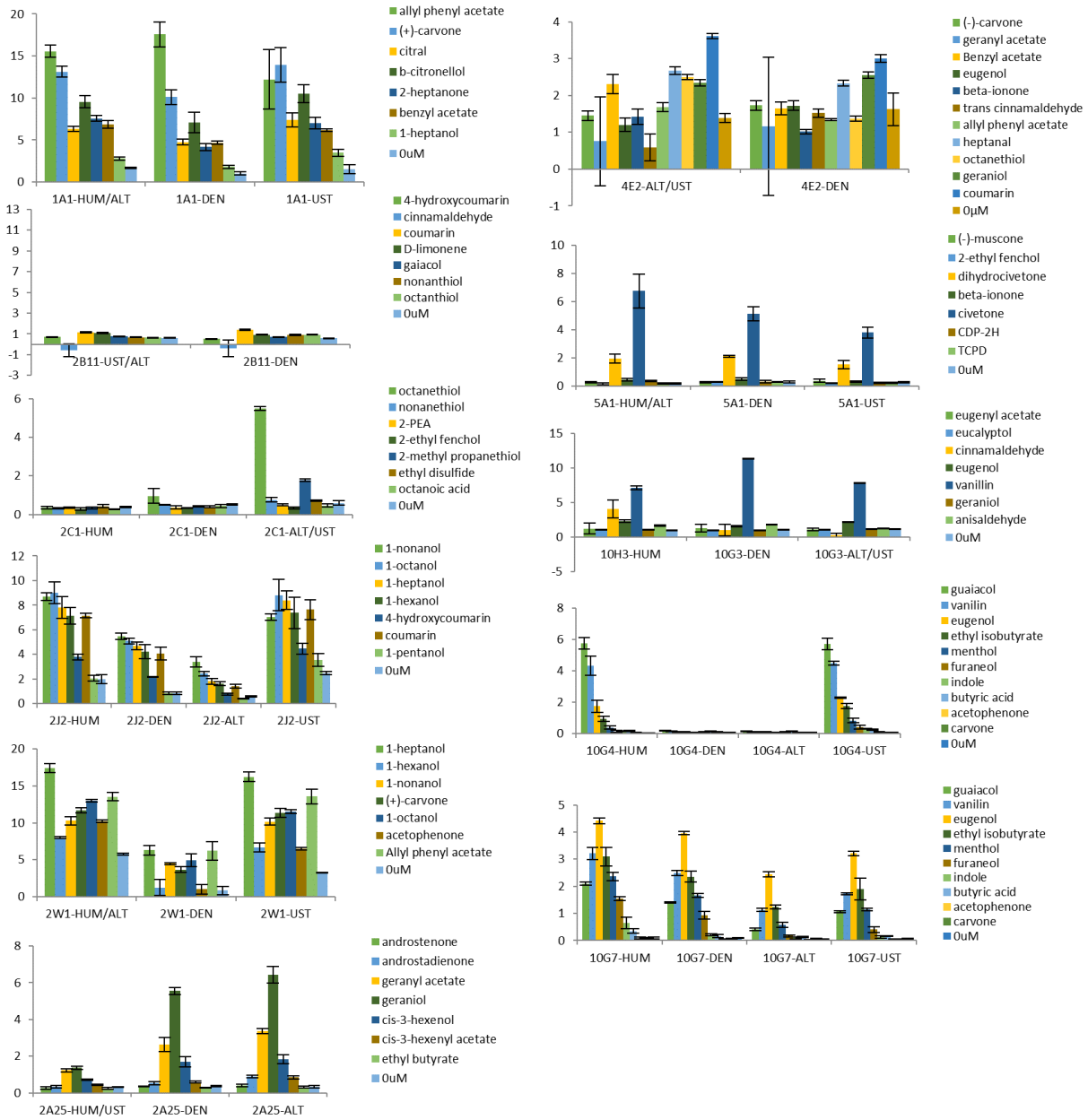

Fig. S6.

Screening of variants identified with the 2013 VCF Data and their corresponding human version response against odorants at 100µM. The y-axis shows normalized luminescence recorded in the luciferase assay.

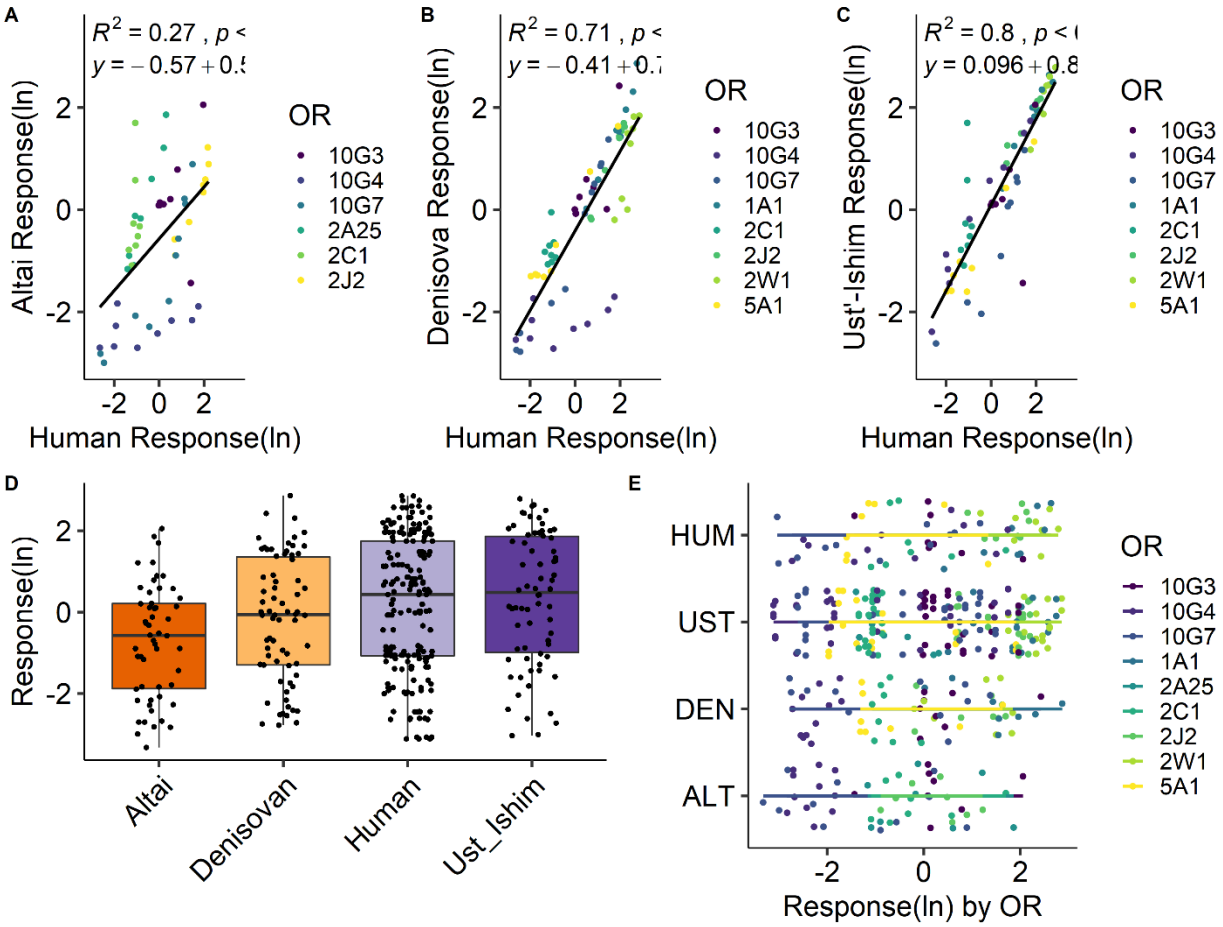

Fig. S7.
Comparison of human (x-axis) and hominin (y-axis) OR responses for **(A)** Altai Neandertal **(B)** Denisova **(C)** Ancient human hunter-gatherer, Ust'-Ishim. **D.** Boxplots of natural log of OR responses across lineages (humans are divided into ancient and modern). **E.** OR response by lineage and gene. Each OR is represented by a different color and each point represents the natural log of the response to an odorant. Dotted lines corresponds to the linear regression for the entire set of ORs responses for a given lineage. The corresponding equation and R^2 values are shown on the regression plot.

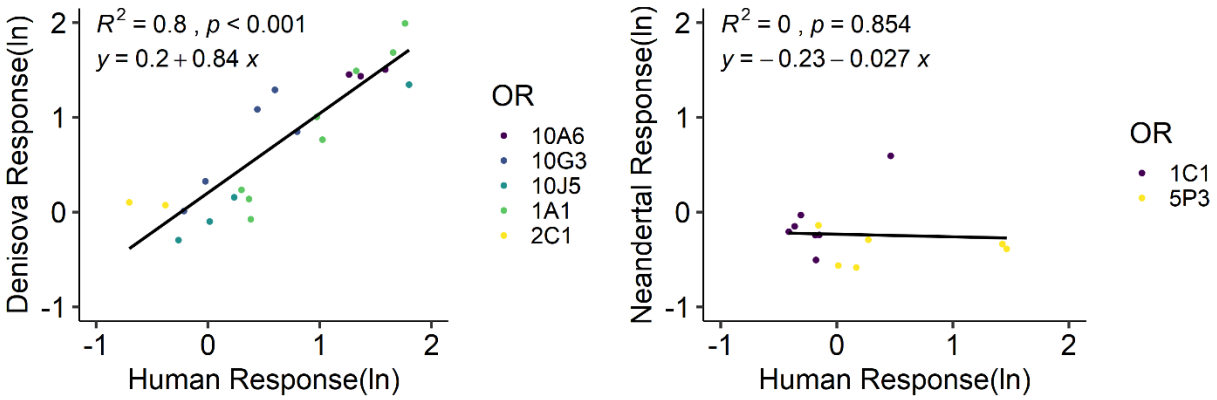

Fig. S8.
Regression results for active ORs only

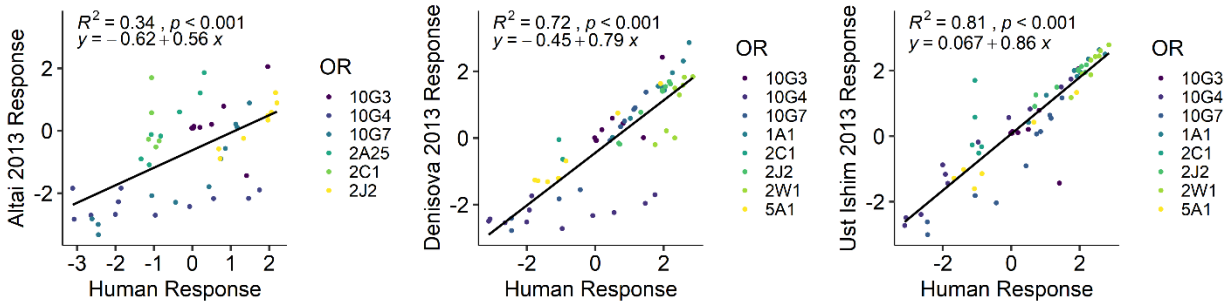

Fig. S9.
Regression results for active ORs only, 2013 data.

Table S1.
Target Genes

Gene	Chr	Region	Odorant	Description
OR6P1	1	158532441-158533394	anisaldehyde	anise, licorice
OR10J5	1	159504868-159505797	lyral	floral, lily
OR2B11	1	247614331-247615284	coumarin	grassy, vanilla, almond
OR1C1	1	247920764-247921708	linalool	floral, bergamot, lavender
OR5K1	3	98188421-98189347	eugenol methyl ether	clove-like
OR2W1	6	29011990-29012952	cis-3-hexen-1-ol	freshly cut grass, leaves
OR2J3	6	29079588-29080603	cinnamaldehyde, cinnamon	cinnamon
OR2J2	6	29141413-29142351	ethyl vanillin	vanilla
OR11A1	6	29394471-29395418	2-ethylfenchol	soil, earth, peat
OR2A25	7	143771313-143772245	geranyl acetate	floral, fruity, rose
OR51E1	11	4673757-4674713	isovaleric acid	sweat, cheese
OR51E2	11	4702979-4703941	androstenone, musk	β-ionone, violet-rose
OR51L1	11	5020213-5021160	allyl phenyl acetate	honey
OR56A4	11	6023281-6024378	undecanal	green coffee, leafy
OR5P3	11	7846584-7847519	coumarin	grassy, vanilla, almond
OR10A6	11	7949265-7950209	3-phenyl propyl propionate	floral balsam hyacinth mimosa
OR8K3	11	56085783-56086721	menthol	mint, menthol
OR5AN1	11	59131932-59132867	muscone	musk
OR5A1	11	59210642-59211589	β-ionone	violet rose
OR10G4	11	123886282-123887217	vanillin	vanilla
OR10G7	11	123908773-123909708	eugenol methyl ether	clove-like (fruits and spices)
OR8D1	11	124179736-124180662	caramel furanone	low-burnt sugar, high-fenugreek/curry
OR8B3	11	124266306-124267247	.+(-) and -(-)carvone	spearmint and carraway
OR4Q3	14	20215587-20216528	eugenol methyl ether	clove-like
OR10G3	14	22037934-22038875	vanillin	vanilla
OR4E2	14	22133297-22134238	n-amyl acetate	bananas, apples
OR2C1	16	3405941-3406879	octanethiol	sulphur
OR1A1	17	3118915-3119844	-(-)carvone	spearmint
OR7D4	19	9324575-9325513	androstenone, adrostadienone	musk
OR7C1	19	14909986-14910948	androstadienone	musk

Table S2.
Materials and Accession Numbers for Ancient Genomic Data

Lineage	Specimen	Location	Date	Accession/DOI
Denisova	Denisova3	Denisovan Cave, Altai Mts, Siberia	74-82K BP	PRJEB3092 10.1126/science.1224344
Neandertal	Altai	Denisovan Cave, Altai Mts, Siberia	50.3 kya ± 2.2	PRJEB1265 10.1038/nature12886
	Chagyrskaya	Chagyrskaya Cave, Altai Mts, Siberia	781-126 kya	eva.mpg.de/neandertal/Chagyrskaya/VCF/ 10.1016/j.aeae.2013.07.002
	Mezmaiskaya1	Mezmaiskaya Cave, Russian Caucasus	60-70 kya	PRJEB21195 10.1126/science.aao1887
	Vindija 33.19	Vindija Cave, Croatia	~50 kya	PRJEB21157 10.1126/science.aao1887
Ancient Human	Ust'-Ishim	Ust'-Ishim District, Western Siberia	49K BP	PRJEB6622 10.1038/nature13810

In the 2016 VCF data, several variants were also found in the earlier 2013 data. A few variants in the 2013 Ust’-Ishim VCF data were not found in the 2016 dataset—due to the damaged DNA genotyper.

Table S3.
1000 Genomes populations

	Group	n
Africa	Esan, Nigeria	99
	Gambian	113
	Luhya, Kenya	99
	Mende, Sierra Leone	85
	Yoruban, Nigeria	108
Asia	Chinese-Beijing Han	103
	Chinese-Southern Han	105
	Chinese-Dai	93
	Japanese	104
	Kinh, Vietnam	99
Southwest Asia	Bengali in Bangladesh	86
	Gujarati, Houston	103
	Punjabi, Pakistan	96
	Tamil (Sri Lanka), UK	102
	Telugu, UK	102
Europe	American White, Utah	99
	British	99
	Finn	99
	Iberian, Spain	107
	Tuscan	107
Americas	American Black	61
	Caribbean Black	91
	Columbian	94
	Mexicans, LA	64
	Peruvian	85
	Puerto Rican	104

Table S4.
Mean of Percentage of Gene/Protein Containing Variants (e.g., n variants/total basepairs per gene or amino acids per protein)

Population	n Genes	%Var/nGenes	%Var/30 genes	n Proteins	%Var	%Var/30 genes
Ancient Denisovan	19	0.21	0.13	16	0.50	0.26
Ancient Neandertal Altai	18	0.18	0.11	12	0.45	0.18
Ancient Neandertal Chagyrskaya	18	0.20	0.12	14	0.45	0.21
Ancient Neandertal Vindija	15	0.18	0.09	11	0.46	0.17
Ancient Ust Ishim	16	0.19	0.10	13	0.39	0.17
Africa Esan	30	1.00	1.00	29	1.85	1.79
Africa Gambian	30	1.05	1.05	30	1.94	1.94
Africa Luhya	30	1.15	1.15	30	2.09	2.09
Africa Mende	30	1.00	1.00	30	1.82	1.82
Africa Yoruban	30	1.08	1.08	30	1.91	1.91
Americas Black USA	30	0.96	0.96	30	1.74	1.74
Americas Black Caribbean	30	1.13	1.13	30	2.04	2.04
Americas Columbian	30	0.88	0.88	29	1.70	1.64
Americas Mexican	30	0.71	0.71	28	1.40	1.30
Americas Peruvian	30	0.75	0.75	29	1.46	1.41
Americas Puerto Rican	30	0.90	0.90	30	1.66	1.66
Americas White USA	30	0.69	0.69	30	1.28	1.28
Asia Dai	30	0.61	0.61	29	1.17	1.14
Asia Han Beijing	30	0.71	0.71	30	1.28	1.28
Asia Han Southern	30	0.69	0.69	30	1.33	1.33
Asia Japanese	30	0.63	0.63	29	1.24	1.20
Asia Kinh	30	0.71	0.71	30	1.37	1.37
Europe British	30	0.68	0.68	30	1.20	1.20
Europe Finn	30	0.63	0.63	29	1.22	1.18
Europe Spanish	30	0.81	0.81	29	1.48	1.43
Europe Tuscan	30	0.77	0.77	30	1.39	1.39
SW Asia Bengali	30	0.78	0.78	29	1.52	1.47
SW Asia Gujarati	30	0.78	0.78	28	1.57	1.46
SW Asia Punjabi	30	0.78	0.78	30	1.47	1.47
SW Asia Tamil	30	0.77	0.77	30	1.39	1.39
SW Asia Telugu	30	0.78	0.78	29	1.51	1.46

Table S5.
Fst based on 30 OR genes for 1000 Genomes and for all high-quality sequences for *Homo* (including 1000 Genomes. Columns are independently ordered in values from high to low.

Gene	Fst: 1KG populations	Gene	Fst: Homo (1000 Genomes and Ancient/Extinct Samples)
OR5P3	0.114	OR7C1	0.445
OR1C1	0.087	OR1C1	0.379
OR10J5	0.068	OR5AN1	0.279
OR8D1	0.063	OR10J5	0.251
OR2B11	0.061	OR51E2	0.244
OR51E1	0.059	OR51E1	0.197
OR56A4	0.058	OR10G3	0.195
OR4E2	0.056	OR8D1	0.185
OR2A25	0.051	OR5A1	0.185
OR2J3	0.043	OR5P3	0.151
OR51E2	0.042	OR2C1	0.133
OR5A1	0.040	OR10A6	0.133
OR7D4	0.037	OR4E2	0.126
OR1A1	0.034	OR2B11	0.091
OR5K1	0.031	OR10G4	0.074
OR2W1	0.029	OR1A1	0.070
OR2J2	0.028	OR8K3	0.046
OR4Q3	0.028	OR56A4	0.036
OR7C1	0.028	OR2J3	0.013
OR10G7	0.028	OR2A25	0.012
OR51L1	0.025	OR2W1	0.008
OR6P1	0.024	OR51L1	0.000
OR8K3	0.024	OR11A1	0.000
OR10G3	0.024	OR2J2	0.000
OR5AN1	0.023	OR10G7	0.000
OR10G4	0.022	OR7D4	0.000
OR11A1	0.022	OR6P1	0.000
OR2C1	0.015	OR4Q3	0.000
OR8B3	0.010	OR5K1	0.000
OR10A6	0.009	OR8B3	0.000
Mean	**0.0394**	**Mean**	0.108

Table S6.
2016 VCF Shared Variants*

Gene	Substitution	Position	RS	Specimen	Quality	Depth	GQ	Note
OR1A1	V233M	17:3119611	rs17762735	Ust'-Ishim	503	39	99	1
OR2A25	A209P	7:143771937	rs2961135	Altai	137	35	99	1
				Chagyrskaya	100	22	99	
				Denisova	108	25	99	1
				Vindija	111	26	99	
OR2A25	S75N	7:143771536	rs6951485	Altai	159	40	99	1
				Chagyrskaya	100	20	99	
				Denisova	99	20	99	1
				Vindija	125	29	99	
OR2B11	S12P	1:247615251	rs147030298	Denisova	108	25	99	1
				Altai	213	30	99	1,2
				Chagyrskaya	106	24	99	2
				Denisova	103	23	99	1,2
OR2C1	C149W	16:3406387	rs1218763	Altai	120	29	99	1
				Chagyrskaya	92	31	92	
				Denisova	128	32	99	1
				Ust'-Ishim	144	39	99	1
				Vindija	108	25	99	
OR2J2	A302V	6:29142317	rs41270628	Altai	116	40	99	1
				Chagyrskaya	111	26	99	
				Vindija	81	16	83	
OR2J2	K312M	6:29142347	rs41270632	Ust'-Ishim	109	27	99	1
OR2J3	R226Q	6:29080344	rs3749977	Denisova	125	29	99	1
OR2W1	D296N	6:29012067	rs35771565	Ust'-Ishim	152	41	99	
OR2W1	P138S	6:29012541	rs146659019	Denisova	124	31	99	
OR4E2	Q234R	14:22133997	rs970382	Altai	149	38	99	1
				Chagyrskaya	126	32	99	
				Denisova	147	38	99	1
				Ust'-Ishim	499	39	99	1
				Vindija	109	27	99	
OR4E2	R233H	14:22133994	rs200419591	Denisova	155	39	99	1
OR4E2	V118M	14:22133648	rs2874103	Altai	201	53	99	1
				Chagyrskaya	99	20	99	
				Denisova	163	41	99	1

				Ust'-Ishim	439	47	99	1
				Vindija	131	31	99	
OR5A1	D183N	11:59211188	rs6591536	Ust'-Ishim	109	25	99	1
OR5A1	G173R	11:59211158	rs140829988	Denisova	306	27	99	1
OR5AN1	L289F	11:59132798	rs7941190	Ust'-Ishim	168	47	99	1
OR7C1	E171K	19:14910438	rs10415312	Altai	205	58	99	1
				Chagyrskaya	155	41	99	
				Denisova	165	45	99	1
				Ust'-Ishim	184	52	99	1
				Vindija	140	37	99	
OR7C1	R233K	19:14910251	rs77999564	Altai	235	67	99	1
				Chagyrskaya	150	39	99	
				Denisova	175	47	99	1
				Vindija	152	40	99	
OR7C1	S210P	19:14910321	rs16979912	Altai	157	52	99	1
				Chagyrskaya	100	24	99	
				Denisova	147	38	99	1
				Vindija	96	21	98	
OR7C1	V126I	19:14910573	rs10415562	Altai	118	28	99	1
				Chagyrskaya	79	15	80	
				Denisova	87	18	89	1
				Ust'-Ishim	118	30	99	1
				Vindija	64	11	66	
OR8K3	L122R	11:56086147	rs960193	Altai	111	26	99	1
				Chagyrskaya	91	19	93	
				Denisova	87	27	87	1
				Ust'-Ishim	141	38	99	1
				Vindija	108	25	99	
OR10A6	L287P	11:7949350	rs4758258	Altai	52	48	53	1
				Chagyrskaya	133	33	99	
				Denisova	156	41	99	1
				Ust'-Ishim	486	43	99	1
				Vindija	92	21	93	
OR10G3	R236Q	14:22038170	rs536842323	Chagyrskaya	152	23	99	
OR10G3	S73G	14:22038659	rs17792778	Altai	131	32	99	1
				Chagyrskaya	79	15	81	
				Denisova	132	33	99	1

				Ust'-Ishim	334	34	99	1
				Vindija	115	27	99	
OR10G4	A9V	11:123886308	rs11219407	Altai	102	23	99	1
				Chagyrskaya	82	16	84	
				Denisova	82	18	83	1
				Ust'-Ishim	12	4	12	1
				Vindija	40	11	40	
OR10G4	A9V	11:123886307	rs79057843	Altai	224	23	99	1
				Chagyrskaya	102	17	99	
				Denisova	205	20	99	1
OR51E1	S11N	11:4673788	rs17224476	Chagyrskaya	105	22	99	
				Vindija	328	36	99	
OR51E1	V205I	11:4674369	rs185465942	Ust'-Ishim	34	32	34	1
OR51L1	A207V	11:5020832	rs10768450	Ust'-Ishim	270	34	99	1
OR51L1	T196I	11:5020799	rs10768448	Ust'-Ishim	446	45	99	1

Gene	**Substitution**	**Position**	**RS**	**Specimen**	**Quality**	**Depth**	**GQ**	**Note**
OR1A1	Synonymous	17:3119008	rs4325604	Altai	169	45	99	1
				Chagyrskaya	93	20	95	
				Denisova	108	25	99	1
				Ust'-Ishim	169	47	99	1
				Vindija	109	31	99	
OR1C1	Synonymous	1:247921352	rs1552813	Altai	139	35	99	1,2
				Chagyrskaya	102	23	99	2
				Denisova	121	29	99	1,2
OR2C1	Synonymous	16:3406516	rs11643487	Altai	124	59	99	1
				Chagyrskaya	115	27	99	1
				Ust'-Ishim	256	35	99	
				Vindija	134	40	99	
OR2W1	Synonymous	6:29012116	rs7341218	Ust'-Ishim	163	43	99	1
OR4E2	Synonymous	14:22133416	rs12717305	Altai	114	37	99	1
				Chagyrskaya	121	29	99	
				Denisova	135	39	99	1
				Ust'-Ishim	665	50	99	1
				Vindija	169	45	99	
OR5A1	Synonymous	11:59211265	rs7941591	Ust'-Ishim	66	28	66	1
OR5P3	Synonymous	11:7847208	rs1482791	Ust'-Ishim	276	31	99	1

OR5P3	Synonymous	11:7847466	rs1482792	Altai	345	51	99	1
				Denisova	168	45	99	1
				Ust'-Ishim	153	51	99	1
OR5P3	Synonymous	11:7847472	rs1482793	Ust'-Ishim	724	53	99	1
OR6P1	Synonymous	1:158533140	rs12080815	Altai	147	38	99	1,2
				Chagyrskaya	91	19	92	2
OR6P1	Synonymous	1:158533224	rs12081915	Altai	175	58	99	1,2
				Chagyrskaya	82	23	82	
OR8D1	Synonymous	11:124179835	rs4936918	Altai	190	52	99	1
				Chagyrskaya	140	35	99	
				Denisova	165	21	99	1
				Vindija	91	19	93	
OR8D1	Synonymous	11:124180082	rs4936919	Altai	126	42	99	1
				Chagyrskaya	133	33	99	
				Denisova	234	22	99	1
				Vindija	104	27	99	
OR10G3	Synonymous	14:22038450	rs11626669	Altai	137	32	99	1
				Chagyrskaya	74	12	75	
				Denisova	102	21	99	1
				Vindija	132	31	99	
OR10G3	Synonymous	14:22038162	rs17197261	Altai	143	45	99	1
				Chagyrskaya	94	20	96	
				Vindija	97	23	97	
OR51E1	Synonymous	11:4674575	rs3817098	Altai	195	52	99	1
				Chagyrskaya	82	14	84	
				Vindija	86	16	87	
OR51E2	Synonymous	11:4703165	rs1123991	Ust'-Ishim	148	38	99	1
OR51L1	Synonymous	11:5020509	rs11035066	Ust'-Ishim	562	48	99	1
OR51L1	Synonymous	11:5020416	rs2445290	Altai	185	54	99	1
				Chagyrskaya	102	27	99	
				Denisova	140	36	99	1
				Ust'-Ishim	223	24	99	1
				Vindija	85	19	86	

***** only one variant was not present in the 2013 dataset

[1] present in 2013 data also
[2] present in 2013 Ust'-Ishim data but not 2016 Ust'-Ishim data

Table S7.
2016 VCF Novel Variants

Gene	Position	Substitution	Sample	Qual	Depth	GQ	Note
OR1A1	17:3119050	V46I	Denisova	142	34	99	1
	17:3119684	T257M	Denisova	141	37	99	1
OR1C1	1:247921351	Y120H	Chagyrskaya	74	23	74	
OR2B11	1:247614839	V149E	Denisova	148	38	99	1
OR2C1	16:3406581	I214T	Denisova	113	27	99	1
OR5P3	11:7847045	F159L	Vindija	87	18	89	
OR6P1	1:158532749	S216A	Altai	174	47	99	1
			Chagyrskaya	85	17	86	
	1:158533360	F12S	Denisova	102	23	99	1
OR10G3	14:22038287	E197K	Denisova	120	29	99	1
OR10J5	1:159505737	G21R	Denisova	142	48	99	

Gene	Position	Synonymous	Sample	Qual	Depth	GQ	Note
OR2B11	1:247615024	V87	Denisova	541	42	99	1
OR5AN1	11:59132645	A238A	Chagyrskaya	22	17	22	
OR10A6	11:7950075	I45I	Denisova	79	26	79	1
OR10G7	11:123908878	T277	Altai	415	51	99	1
			Chagyrskaya	128	20	99	
			Vindija	96	19	98	

[1] present in 2013 data also
[2] present in 2013 Ust'-Ishim data but not 2016 Ust'-Ishim data

Table S8.
2013 VCF Variants

Specimen	Gene	Position	RS	Quality	Raw Read Depth	Mapping Quality	Type
Altai	OR6P1	1:158532749	Novel	228	48	37	S216A
Altai	OR6P1	1:158533140	rs12080815	228	42	39	SYNON
Ust'-Ishim	OR6P1	1:158533140	rs12080815	228	33	36	SYNON
Altai	OR6P1	1:158533224	rs12081915	228	62	37	SYNON
Ust'-Ishim	OR6P1	1:158533224	rs12081915	228	41	37	SYNON
Denisova	OR6P1	1:158533360	Novel	228	20	37	F12S
Ust'-Ishim	OR10J5	1:159505297	rs4656837	222	41	37	SYNON
Denisova	OR10J5	1:159505737	Novel	228	44	37	G21R
Altai	OR2B11	1:247614693	rs6695302	161	33	38	V198M
Denisova	OR2B11	1:247614693	rs6695302	228	23	37	V198M
Ust'-Ishim	OR2B11	1:247614693	rs6695302	228	34	37	V198M
Denisova	OR2B11	1:247614839	Novel	228	37	37	V149E
Altai	OR2B11	1:247614896	rs11583410	228	30	37	I130S
Denisova	OR2B11	1:247614896	rs11583410	228	25	37	I130S
Ust'-Ishim	OR2B11	1:247614896	rs11583410	228	20	37	I130S
Denisova	OR2B11	1:247615024	Novel	222	39	37	SYNON
Denisova	OR2B11	1:247615251	rs147030298	228	25	37	S12P
Ust'-Ishim	OR1C1	1:247921100	rs1552812	228	36	37	SYNON
Altai	OR1C1	1:247921352	rs1552813	228	37	38	SYNON
Denisova	OR1C1	1:247921352	rs1552813	228	29	37	SYNON
Ust'-Ishim	OR1C1	1:247921352	rs1552813	228	33	37	SYNON
Ust'-Ishim	OR5K1	3:98188365	rs9861575	182	50	37	W14C
Ust'-Ishim	OR2W1	6:29012067	rs35771565	228	42	38	D296N
Ust'-Ishim	OR2W1	6:29012116	rs7341218	228	44	38	SYNON
Denisova	OR2W1	6:29012541	rs146659019	228	31	37	P138A
Denisova	OR2J3	6:29080344	rs3749977	228	27	37	R226Q
Altai	OR2J3	6:29080349	rs3130764	228	36	36	I228V
Denisova	OR2J3	6:29080349	rs3130764	228	26	35	I228V
Altai	OR2J3	6:29080450	rs3130765	228	44	31	M261I/M
Denisova	OR2J3	6:29080450	rs3130765	228	35	26	M261I/M
Altai	OR2J2	6:29141772	rs3129158	228	50	31	SYNON
Denisova	OR2J2	6:29141772	rs3129158	203	20	28	SYNON
Altai	OR2J2	6:29142317	rs41270628	228	44	37	A302V
Ust'-Ishim	OR2J2	6:29142347	rs41270632	228	31	34	K312M
Altai	OR2A25	7:143771536	rs6951485	228	45	35	S75N

Denisova	OR2A25	7:143771536	rs6951485	228	22	33	S75N
Denisova	OR2A25	7:143771733	Novel	136	32	37	I141V
Altai	OR2A25	7:143771937	rs2961135	228	43	38	A209P
Denisova	OR2A25	7:143771937	rs2961135	228	25	37	A209P
Ust'-Ishim	OR51E1	11:4674369	rs185465942	33	32	37	V205I
Altai	OR51E1	11:4674575	rs3817098	228	56	37	SYNON
Ust'-Ishim	OR51E2	11:4703165	rs1123991	228	39	37	SYNON
Altai	OR51L1	11:5020416	rs2445290	228	60	38	SYNON
Denisova	OR51L1	11:5020416	rs2445290	228	36	37	SYNON
Ust'-Ishim	OR51L1	11:5020416	rs2445290	156	24	37	SYNON
Ust'-Ishim	OR51L1	11:5020509	rs11035066	222	52	36	SYNON
Ust'-Ishim	OR51L1	11:5020799	rs10768448	222	45	36	T196I
Ust'-Ishim	OR51L1	11:5020832	rs10768450	222	37	37	A207V
Altai	OR5P3	11:7846722	Novel	222	46	37	Y266STOP
Altai	OR5P3	11:7846752	Novel	222	52	37	SYNON
Ust'-Ishim	OR5P3	11:7847208	rs1482791	157	32	37	SYNON
Altai	OR5P3	11:7847466	rs1482792	222	55	39	SYNON
Denisova	OR5P3	11:7847466	rs1482792	228	44	37	SYNON
Ust'-Ishim	OR5P3	11:7847466	rs1482792	228	54	36	SYNON
Ust'-Ishim	OR5P3	11:7847472	rs1482793	222	56	36	SYNON
Altai	OR10A6	11:7949350	rs4758258	228	54	39	SYNON
Denisova	OR10A6	11:7949350	rs4758258	228	42	37	SYNON
Ust'-Ishim	OR10A6	11:7949350	rs4758258	222	45	38	SYNON
Ust'-Ishim	OR10A6	11:7950024	rs12272735	183	28	34	SYNON
Denisova	OR10A6	11:7950075	Novel	228	26	37	SYNON
Altai	OR8K3	11:56086147	rs960193	228	29	38	L122R
Denisova	OR8K3	11:56086147	rs960193	228	24	35	L122R
Ust'-Ishim	OR8K3	11:56086147	rs960193	228	41	36	L122R
Ust'-Ishim	OR5AN1	11:59132798	rs7941190	228	50	37	L289F
Denisova	OR5A1	11:59211158	rs140829988	222	29	37	G173R
Ust'-Ishim	OR5A1	11:59211188	rs6591536	228	25	37	D183N
Ust'-Ishim	OR5A1	11:59211265	rs7941591	228	28	37	SYNON
Altai	OR10G4	11:123886307	rs79057843	175	43	28	A9V
Denisova	OR10G4	11:123886307	rs79057843	160	25	32	A9V
Altai	OR10G4	11:123886308	rs11219407	228	43	28	A9V
Denisova	OR10G4	11:123886308	rs11219407	228	25	32	A9V
Ust'-Ishim	OR10G4	11:123886308	rs11219407	89	11	21	A9V
Ust'-Ishim	OR10G4	11:123886320	Novel	88	7	19	T13A

Altai	OR10G4	11:123886681	Novel	193	59	14	M134V
Denisova	OR10G4	11:123886681	Novel	44	33	10	M134V
Altai	OR10G4	11:123886865	rs4084209	228	31	33	V195E
Denisova	OR10G4	11:123886865	rs4084209	228	19	30	V195E
Ust'-Ishim	OR10G4	11:123886865	rs4084209	228	21	28	V195E
Denisova	OR10G4	11:123886948	Novel	50	32	17	S223T
Denisova	OR10G4	11:123886950	Novel	76	32	17	S223T
Altai	OR10G4	11:123886984	rs4936880	221	50	34	R235G
Denisova	OR10G4	11:123886984	rs4936880	228	19	36	R235G
Altai	OR10G4	11:123887164	rs4936881	228	32	25	K295Q
Denisova	OR10G4	11:123887164	rs4936881	205	17	22	K295Q
Altai	OR10G4	11:123887184	rs4936882	228	28	33	SYNON
Denisova	OR10G4	11:123887184	rs4936882	228	23	34	SYNON
Ust'-Ishim	OR10G4	11:123887184	rs4936882	228	33	33	SYNON
Altai	OR10G7	11:123908878	Novel	222	55	37	SYNON
Altai	OR10G7	11:123908977	rs188316662	143	54	15	SYNON
Denisova	OR10G7	11:123909073	rs11219419	29	30	23	SYNON
Ust'-Ishim	OR10G7	11:123909073	rs11219419	228	25	27	SYNON
Altai	OR10G7	11:123909099	rs59358830	222	37	37	L204I
Ust'-Ishim	OR10G7	11:123909172	rs28414940	74	43	8	SYNON
Altai	OR10G7	11:123909302	rs513591	175	41	33	T136S
Denisova	OR10G7	11:123909302	rs513591	150	17	34	T136S
Altai	OR10G7	11:123909311	rs472442	75	32	30	N133S
Denisova	OR10G7	11:123909311	rs472442	126	15	34	N133S
Ust'-Ishim	OR10G7	11:123909342	rs470242	200	12	27	SYNON
Altai	OR10G7	11:123909637	Novel	70	8	34	SYNON
Ust'-Ishim	OR10G7	11:123909650	rs3894199	111	32	17	G20A
Altai	OR10G7	11:123909653	rs4998340	29	17	22	P19Q
Ust'-Ishim	OR10G7	11:123909653	rs4998340	135	31	18	P19Q
Altai	OR10G7	11:123909656	rs3894198	20	21	21	A18L
Denisova	OR10G7	11:123909656	rs3894198	10	7	19	A18L
Ust'-Ishim	OR10G7	11:123909656	rs3894198	128	28	17	A18L
Altai	OR10G7	11:123909671	rs11827843	113	27	23	T13M
Denisova	OR10G7	11:123909671	rs11827843	47	16	20	T13M
Altai	OR10G7	11:123909695	rs3894197	203	38	35	T5S
Denisova	OR10G7	11:123909695	rs3894197	87	15	26	T5S
Ust'-Ishim	OR10G7	11:123909695	rs3894197	228	24	29	T5S
Altai	OR8D1	11:124179835	rs4936918	228	53	37	SYNON

Denisova	OR8D1	11:124179835	rs4936918	126	19	37	SYNON
Altai	OR8D1	11:124180082	rs4936919	228	45	38	SYNON
Denisova	OR8D1	11:124180082	rs4936919	193	20	37	SYNON
Ust'-Ishim	OR8B3	11:124266906	Novel	221	64	26	SYNON
Altai	OR8B3	11:124266912	rs28398895	228	55	33	SYNON
Denisova	OR8B3	11:124266912	rs28398895	228	34	34	SYNON
Ust'-Ishim	OR8B3	11:124266912	rs28398895	220	61	27	SYNON
Altai	OR8B3	11:124267056	rs144478570	38	61	12	SYNON
Denisova	OR8B3	11:124267056	rs144478570	15	63	12	SYNON
Denisova	OR8B3	11:124267189	rs507335	10	9	2	H20R
Altai	OR4Q3	14:20216298	rs12896533 [1]	228	35	29	F238L
Denisova	OR4Q3	14:20216298	rs12896533 [1]	228	24	28	F238L
Ust'-Ishim	OR4Q3	14:20216298	rs12896533 [1]	228	33	27	F238L
Altai	OR10G3	14:22038162	rs17197261	228	51	38	SYNON
Denisova	OR10G3	14:22038287	Novel	228	27	37	SYNON
Altai	OR10G3	14:22038450	rs11626669	228	35	39	SYNON
Denisova	OR10G3	14:22038450	rs11626669	228	17	37	SYNON
Ust'-Ishim	OR10G3	14:22038525	rs11626693	222	50	37	SYNON
Altai	OR10G3	14:22038659	rs17792778	228	37	39	S73G
Denisova	OR10G3	14:22038659	rs17792778	228	29	37	S73G
Ust'-Ishim	OR10G3	14:22038659	rs17792778	222	36	36	S73G
Altai	OR4E2	14:22133416	rs12717305	228	40	38	SYNON
Denisova	OR4E2	14:22133416	rs12717305	228	38	37	SYNON
Ust'-Ishim	OR4E2	14:22133416	rs12717305	222	51	37	SYNON
Altai	OR4E2	14:22133648	rs2874103	228	57	39	V118M
Denisova	OR4E2	14:22133648	rs2874103	228	40	37	V118M
Ust'-Ishim	OR4E2	14:22133648	rs2874103	222	47	37	V118M
Denisova	OR4E2	14:22133994	rs200419591	228	29	37	R233H
Altai	OR4E2	14:22133997	rs970382	228	39	37	Q234R
Denisova	OR4E2	14:22133997	rs970382	228	31	37	Q234R
Ust'-Ishim	OR4E2	14:22133997	rs970382	222	39	37	Q234R
Altai	OR2C1	16:3405994	rs1228348	228	62	38	SYNON
Ust'-Ishim	OR2C1	16:3405994	rs1228348	165	27	37	SYNON
Altai	OR2C1	16:3406387	rs1218763	228	33	37	C149W
Denisova	OR2C1	16:3406387	rs1218763	228	31	37	C149W
Ust'-Ishim	OR2C1	16:3406387	rs1218763	228	41	37	C149W
Altai	OR2C1	16:3406516	rs11643487	228	59	37	SYNON
Ust'-Ishim	OR2C1	16:3406516	rs11643487	146	36	37	SYNON

Denisova	OR2C1	16:3406581	Novel	228	29	37	I214T
Altai	OR1A1	17:3119008	rs4325604	228	46	36	SYNON
Denisova	OR1A1	17:3119008	rs4325604	228	19	37	SYNON
Ust'-Ishim	OR1A1	17:3119008	rs4325604	228	48	37	SYNON
Denisova	OR1A1	17:3119050	Novel	228	30	37	V46I
Denisova	OR1A1	17:3119383	Novel	228	40	37	L157F
Altai	OR1A1	17:3119397	rs769425	228	59	37	SYNON
Ust'-Ishim	OR1A1	17:3119397	rs769425	222	39	35	SYNON
Ust'-Ishim	OR1A1	17:3119611	rs17762735	222	40	37	V233M
Denisova	OR1A1	17:3119684	Novel	228	27	37	T257M
Denisova	OR7D4	19:9324904	rs546470301	221	35	26	A204T
Denisova	OR7D4	19:9324971	Novel	139	36	31	SYNON
Altai	OR7C1	19:14910251	rs77999564	228	66	37	R233K
Denisova	OR7C1	19:14910251	rs77999564	228	43	37	R233K
Altai	OR7C1	19:14910321	rs16979912	228	55	37	S210P
Denisova	OR7C1	19:14910321	rs16979912	228	38	37	S210P
Altai	OR7C1	19:14910438	rs10415312	228	58	37	E171K
Denisova	OR7C1	19:14910438	rs10415312	228	36	37	E171K
Ust'-Ishim	OR7C1	19:14910438	rs10415312	228	52	37	E171K
Altai	OR7C1	19:14910573	rs10415562	228	36	36	V126I
Denisova	OR7C1	19:14910573	rs10415562	228	24	33	V126I
Ust'-Ishim	OR7C1	19:14910573	rs10415562	228	44	31	V126I

[1] rs12896533 is no longer considered valid (AKA rs61086986)

Table S9.
Novel 2013 VCF Variants

Specimen	Gene	Position	RS	Quality	Raw Read Depth	Mapping Quality	Type
Altai	OR10G4	11:123886681	Novel	193	59	14	M134V
Altai	OR10G7	11:123908878	Novel	222	55	37	SYNON
Altai	OR10G7	11:123909637	Novel	70	8	34	SYNON
Altai	OR5P3	11:7846722	Novel	222	46	37	Y266STOP
Altai	OR5P3	11:7846752	Novel	222	52	37	SYNON
Altai	OR6P1	1:158532749	Novel	228	48	37	S216A
Denisova	OR10A6	11:7950075	Novel	228	26	37	SYNON
Denisova	OR10G3	14:22038287	Novel	228	27	37	SYNON
Denisova	OR10G4	11:123886681	Novel	44	33	10	M134V
Denisova	OR10G4	11:123886948	Novel	50	32	17	S223T
Denisova	OR10G4	11:123886950	Novel	76	32	17	S223T
Denisova	OR10J5	1:159505737	Novel	228	44	37	G21R
Denisova	OR1A1	17:3119050	Novel	228	30	37	V46I
Denisova	OR1A1	17:3119383	Novel	228	40	37	L157F
Denisova	OR1A1	17:3119684	Novel	228	27	37	T257M
Denisova	OR2A25	7:143771733	Novel	136	32	37	I141V
Denisova	OR2B11	1:247614839	Novel	228	37	37	V149E
Denisova	OR2B11	1:247615024	Novel	222	39	37	SYNON
Denisova	OR2C1	16:3406581	Novel	228	29	37	I214T
Denisova	OR6P1	1:158533360	Novel	228	20	37	F12S
Denisova	OR7D4	19:9324971	Novel	139	36	31	SYNON
Ust'-Ishim	OR10G4	11:123886320	Novel	88	7	19	T13A
Ust'-Ishim	OR8B3	11:124266906	Novel	221	64	26	SYNON

Data S1. (separate file)
Raw data and codes for this project and data derived from it are available in at https://github.com/kchoover14/OldNoses and are usable under the license provided in the repository.